Supplementary Information: Correlating geminal $^2J_{\text{Si-O-Si}}$ couplings to structure in framework silicates.

D. J. Srivastava[a], P. Florian[b], J. H. Baltisberger[c] and P. J. Grandinetti*[a1]
[a] *Department of Chemistry and Biochemistry, 100 West 18th Avenue, Columbus, OH, USA. E-mail: grandinetti.1@osu.edu*
[b] *CNRS, UPR3079 CEMHTI, 1D Avenue de la Recherche Scientifique, 45071 Orléans Cedex 2, France.*
[c] *Division of Natural Science, Mathematics, and Nursing, Berea College, Berea, KY, USA.*

S1. GAUSSIAN INTEGRATION GRID SIZE

The effect of change in $^2J_{\text{Si-O-Si}}$ coupling evaluation with the size of the integration grid was tested to avoid integration errors. A series of calculations were run with (*1*) *'fine'*, pruned (75, 302) and (*2*) *'ultrafine'*, pruned (99, 590) integration grids. As seen in Fig. S1, no difference in the $^2J_{\text{Si-O-Si}}$ coupling was observed with the increase in the integration grid size. Thus, all remaining calculations were run with *'fine'* integration grid.

S2. CONTRIBUTIONS TO THE NET J COUPLING

The net J-coupling includes contributions from Fermi contact (FC), Spin-dipolar (SD), paramagnetic spin-orbit (PSO) and diamagnetic spin-orbit (DSO).

$$J = J_{\text{FC}} + J_{\text{SD}} + J_{\text{PSO}} + J_{\text{DSO}}$$

For $^2J_{\text{Si-O-Si}}$ couplings—calculated using Gaussian 09[1] with high level of theory—across a Si-O-Si linkage, the net J-coupling is dominated by the Fermi contact term. As shown in Fig. S2, the combined contribution from SD, PSO, DSO terms account to less than 10% of the contribution from net J-coupling. The combined contribution increases slightly around indexes 1 to 10, indexes 52-67 and indexes 108, 114, 120 and 126, and is associated with clusters with lower Si-O-Si bond angles, Ω_0 in the range of 120° to 130°.

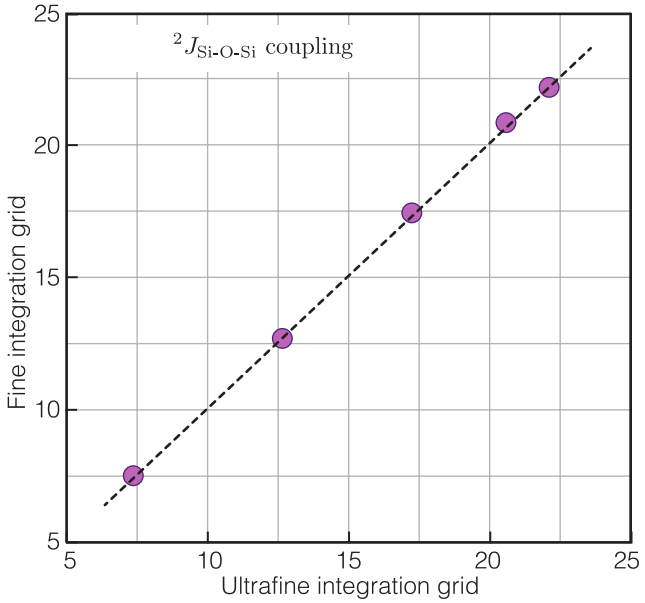

FIG. S1. A perfect correlation of $^2J_{\text{Si-O-Si}}$ coupling evaluated from *'fine'* and *'ultrafine'* integration grid.

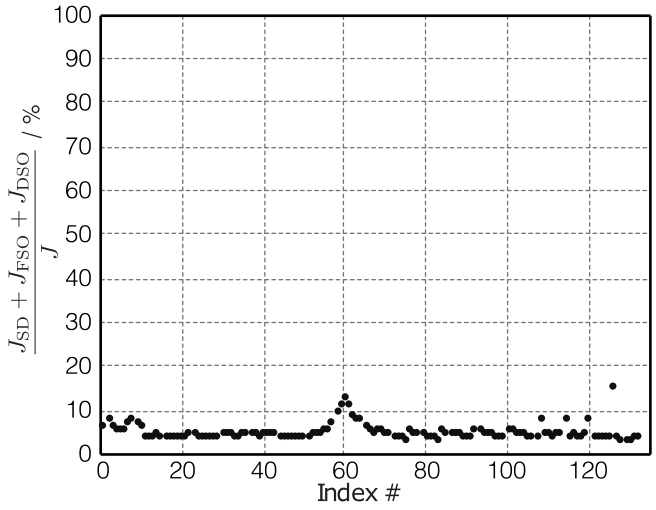

FIG. S2. Combined contribution from SD, PSO and DSO terms accounts to less that 10% of the net J-coupling. The horizontal axis—labeled as index—refer to the index number in Table S1-S3.

S3. S-CHARACTER MODEL

A. s-character at the Si HTO along Si-O bond

In cluster calculations with all the Si-O bond distances fixed at $d_{\text{Si-O}} = 1.6$ Å and with all intra-tetrahedral-angles fixed at $\angle$O-Si-O = 109.5°, we found that the a^2_{Si} of a given Si-O bond depends not only on the Si-O-Si bond angle of its linkage, but also on the other three Si-O-Si bond angles around the silicon. As explained in the main text this arises because the sum of a^2_{Si} from all four Si-O bonds about the Si tetrahedron must remain constant. A strong correlation between a^2_{Si} of a given Si-O bond and the four surrounding Si-O-Si bond angles was found to be

$$a^2_{\text{Si}} \approx c_{\text{Si}} + m_{\text{Si}} \left(\cos\Omega_0 - \cos\langle\Omega\rangle\right), \qquad (1)$$

where $m_{\text{Si}} = 0.0279$, $c_{\text{Si}} = 0.2465$ with $R^2 = 0.96894$. The *ab-initio*-derived data supporting this correlation are

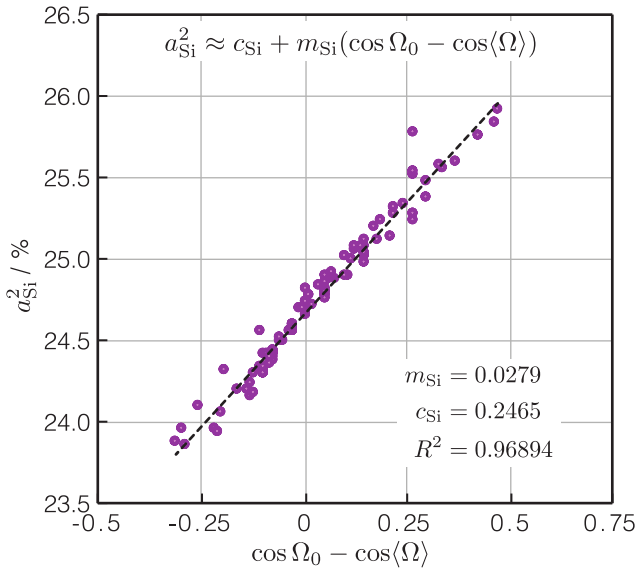

FIG. S3. Variation in the s-character at Si HTO along the Si-O bond as the function of the Si-O-Si tetrahedral angle Ω_0 and average Si-O-Si bond angle, $\langle\Omega\rangle$.

shown in Fig. S3. From Eq. (1), it follows that when all four Si-O-Si bond angles about the Si tetrahedron are equal, the s-character along all four Si-O bonds are also equal.

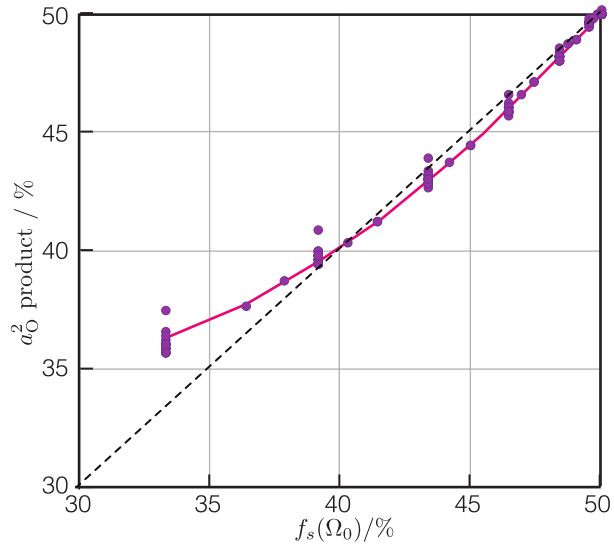

FIG. S4. Comparison of the s-character at bridging oxygen HTO along the Si-O bond against the popular[2,3] approximation $f_s(\Omega_0)$.

B. s-character at the bridging O HTO along Si-O bond

The popular[2,3] approximation of the s-character at the bridging oxygen along the Si-O bond follows,

$$f_s(\Omega_0) = \frac{\cos\Omega_0}{\cos\Omega_0 - 1}. \tag{2}$$

Although the approximation in Eq. (2) gives a good agreement with respect to *ab-initio* calculated s-character, $a^2_{\rm O}$, at higher Ω_0, we shown in Fig. S4 that this agreement appears to break at lower Ω_0.

S4. ^{29}SI ISOTROPIC CHEMICAL SHIFT

In 1983, Smith and Blackwell[4] first showed a correlation between the ^{29}Si isotropic chemical shift, δ_{CS}, and the average secant of the four Si-O-Si bond angles, Ω, about a Si tetrahedron given by

$$\delta_{CS} = a'_\delta\ \langle\sec\Omega\rangle + b'_\delta. \tag{3}$$

Later, the same year, Thomas *et. al.*[5] showed that ^{29}Si isotropic chemical shift correlate linearly with $\langle\Omega\rangle$, according to

$$\delta_{CS} = a_\delta\ \langle\Omega\rangle + b_\delta. \tag{4}$$

The two models, stating different apparent correlations, both showed a good agreement with experiment. In 1984, Engelhardt and Radeglia[3], with the assumption that the chemical shift is dominated by paramagnetic contribution, described ^{29}Si isotropic chemical shift using a simple quantum mechanical model to follow

$$\delta_{CS} = A_\delta \sum_{n=1}^{4} f_{\rm O}(\Omega_n) + B_\delta. \tag{5}$$

The authors showed that the reason Eqs. (3)-(5) all show a good agreement with experiment is that the weak curvature of both $f_{\rm O}(\Omega)$ and $\sec\Omega$ in the relevant range of about 140°-160° cause the ^{29}Si isotropic chemical shift to remain mostly linear with respect to the average Si-O-Si bond angle, $\langle\Omega\rangle$. Many other models[6] have since been proposed, however, by far the simplest correlation is given by Thomas *et. al.*[5], which can be derived by performing a Taylor series expansion of Eq. (5) about 150° with coefficients

$$a_\delta = 1.0025 \times 10^{-2} A_\delta \text{ and } b_\delta = 0.3527\ A_\delta + B_\delta.$$

The coefficient $A_\delta = -61.7625$ ppm/° and $B_\delta = 2.19$ ppm from Engelhardt and Radeglia[3] yields $a_\delta = -0.6191$ ppm/° and $b_\delta = -19.593$ ppm which is within 1.5% of the linear fit reported in the main document.

S5. J-COUPLING AS A FUNCTION OF Ω_0

Cadars *et. al.*[7] discussed the scattering of $^2J_{\text{Si-O-Si}}$ coupling as a function of the central linkage angle Ω_0 resulting from the local structural variations about the central

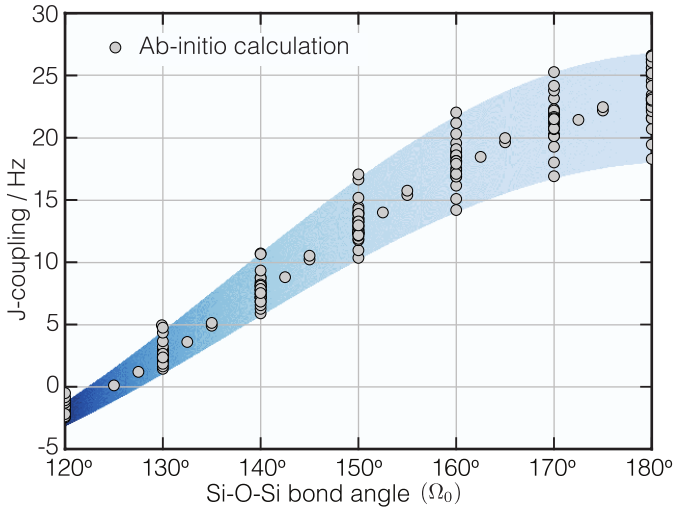

FIG. S5. Scattering of ^2J-coupling as a function of central Si-O-Si linkage angle Ω_0 arising from the variation is local structure around the central Si-O-Si linkage, specially the double average $\overline{\langle\Omega\rangle}$. The gray dots are the *ab-initio* calculated ^2J-couplings and the background image is the intensity plot of ^2J-coupling assuming a uniform distribution of $\overline{\langle\Omega\rangle}$.

Si-O-Si linkage. In Fig. S5 we show the extent of this scattering as a function of Ω_0. The gray dots are the *ab-initio* calculated J-couplings—presented in Table S1-S4—and the image in the background is calculated using Eq. (19) from the main document—assuming a uniform distribution of $\overline{\langle\Omega\rangle}$. A significant scatter of J-coupling is observed when only considering the center linkage angle Ω_0—specially at higher Ω_0.

S6. J-COUPLING MODEL APPROXIMATION

In the main text, we described an analytical expression for calculating the Si-O-Si bond angle

$$\Omega_0(x) = \frac{180^\circ}{\pi}\cos^{-1}\left[-\frac{1}{3}x + \{S(x)+T(x)\}\right], \qquad (6)$$

where

$$\begin{aligned} S(x) &= \sqrt[3]{R(x)+\sqrt{D(x)}},\\ T(x) &= \sqrt[3]{R(x)-\sqrt{D(x)}},\\ D(x) &= \frac{1}{108}x^2\left(4x+27\right),\\ R(x) &= -\frac{1}{54}x\left(2x^2+18x+27\right) \text{ and}\\ x &= \frac{J-J_0}{m_1\overline{\langle\Omega\rangle}}. \end{aligned}$$

Due to the overly complicated parameterization of Eq. (6), we approximated Eq. (6) by

$$g(x) = a_j + b_j\ x + c_j\ \exp\{d_j\ x\} \qquad (8)$$

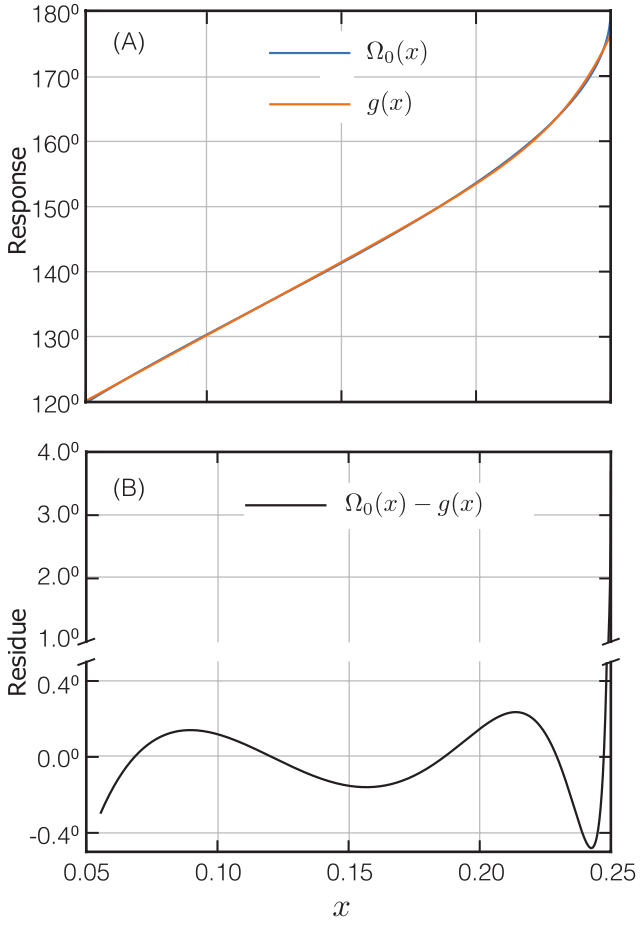

FIG. S6. (A) Comparison of $\Omega_0(x)$ and $g(x)$ as a function of $x \in [1/18, 1/4]$. A good agreement between $g(x)$ and $\Omega_0(x)$ is observed within the range corresponding to $\Omega_0 \in [120°, 176°]$ shown in (B).

where the coefficients $a_j = 107.88°$, $b_j = 223.49°$, $c_j = 0.00002487°$ and $d_j = 53.01$ were determined from the least square minimization. In Fig. S6, we show the comparison between $\Omega_0(x)$ and $g(x)$. A good agreement is observed for the range of x corresponding to $\Omega_0(x) \in [120°, 176°]$ to within $\pm 0.5°$. The deviation at 176° and onwards is significant to a maximum of 3.7° at $\Omega_0(x) = 180°$. However, due to the low probability of Si-O-Si bond angles in this range $[176°, 180°]$, this deviation has been neglected in our study.

[1] M. J. Frisch, G. W. Trucks, H. B. Schlegel, G. E. Scuseria, M. A. Robb, J. R. Cheeseman, G. Scalmani, V. Barone, B. Mennucci, G. A. Petersson, H. Nakatsuji, M. Caricato, X. Li, H. P. Hratchian, A. F. Izmaylov, J. Bloino, G. Zheng, J. L. Sonnenberg, M. Hada, M. Ehara, K. Toyota, R. Fukuda, J. Hasegawa, M. Ishida, T. Nakajima, Y. Honda, O. Kitao, H. Nakai, T. Vreven, J. A. M. Jr., J. E. Peralta, F. Ogliaro, M. J. Bearpark, J. J. Heyd, E. N. Brothers, K. N. Kudin, V. N. Staroverov, T. A. Keith, R. Kobayashi, J. Normand, K. Raghavachari, A. P. Rendell, J. C. Burant, S. S. Iyengar, J. Tomasi, M. Cossi, N. Rega, J. M. Millam, M. Klene, J. E. Knox, J. B. Cross, V. Bakken, C. Adamo, J. Jaramillo, R. Gomperts, R. E. Stratmann, O. Yazyev, A. J. Austin, R. Cammi, C. Pomelli, J. W. Ochterski, R. L. Martin, K. Morokuma, V. G. Zakrzewski, G. A. Voth, P. Salvador, J. J. Dannenberg, S. Dapprich, A. D. Daniels,

O. Farkas, J. B. Foresman, J. V. Ortiz, J. Cioslowski, D. J. Fox, Gaussian 09 Revision D.01 (2013).

[2]M. Klessigner, M. Barfield, The structural dependence of geminal ^{13}C–^{13}C coupling constants, Ellis Horwood, Chichester, 1987, Ch. 16, pp. 269–284.

[3]G. Engelhardt, R. Radeglia, A semi-empirical quantum-chemical rationalization of the correlation between SiOSi angles and ^{29}Si NMR chemical shifts of silica polymorphs and framework aluminosilicates (zeolites), Chemical Physics Letters 108 (1984) 271 – 274. doi:10.1016/0009-2614(84)87063-3.

[4]J. V. Smith, C. S. Blackwell, Nuclear magnetic resonance of silica polymorphs, Nature 303 (1983) 223 – 225. doi:10.1038/303223a0.

[5]J. Thomas, J. Klinowski, S. Ramdas, B. Hunter, D. Tennakoon, The evaluation of non-equivalent tetrahedral sites from ^{29}Si NMR chemical shifts in zeolites and related aluminosilicates, Chemical Physics Letters 102 (1983) 158 – 162. doi:10.1016/0009-2614(83)87384-9.

[6]F. Mauri, A. Pasquarello, B. G. Pfrommer, Y.-G. Yoon, S. G. Louie, Si-O-Si bond-angle distribution in vitreous silica from first-principles ^{29}Si NMR analysis, Phys. Rev. B 62 (8) (2000) 4786–4789.

[7]S. Cadars, D. H. Brouwer, B. F. Chmelka, Probing local structures of siliceous zeolite frameworks by solid-state NMR and first-principles calculations of ^{29}Si-O-^{29}Si scalar couplings, Phys. Chem. Chem. Phys. 11 (2009) 1825–1837. doi:10.1039/b815361b.

TABLE S1. *ab-initio* calculated vs $^2J_{\text{Si-O-Si}}$ coupling model $J(\Omega_0, \overline{\langle\Omega\rangle}, \phi)$ and $J(\Omega_0, \overline{\langle\Omega\rangle})$, Eq. (17) and (19) respectively of the main document, as a function of local parameters including Ω, $\overline{\langle\Omega\rangle}$ and ϕ. The initial geometry was optimized with RHF/6-311G(d). Individual geometry, after structural constraint on Ω_0, Ω_k and ϕ, was not optimized. All Si-O bond distances were fixed to 1.6 Å and O-Si-O intra-tetrahedral angle set to 109.5°.

Index	$\Omega_0/1^\circ$	$\Omega_k/1^\circ$						$\overline{\langle\Omega\rangle}/1^\circ$	$\phi/1^\circ$	$^2J_{\text{Si-O-Si}}$-coupling /Hz		
		Ω_1	Ω_2	Ω_3	Ω_4	Ω_5	Ω_6			*ab-initio*	$J(\Omega_0, \overline{\langle\Omega\rangle}, \phi)$	$J(\Omega_0, \overline{\langle\Omega\rangle})$
1	120	146	146	146	146	146	146	139.5	-59.837	-1.8738	-1.7949	-2.1819
2	120	146	146	146	146	146	146	139.5	-45.539	-1.4292	-1.9006	-2.1819
3	120	146	146	146	146	146	146	139.5	-20.286	-1.8025	-2.3703	-2.1819
4	120	146	146	146	146	146	146	139.5	8.237	-1.9657	-2.5334	-2.1819
5	120	146	146	146	146	146	146	139.5	36.126	-1.9524	-2.0598	-2.1819
6	130	146	146	146	146	146	146	142	-42.783	3.0394	2.9474	2.6332
7	130	146	146	146	146	146	146	142	-18.639	2.4312	2.3494	2.6332
8	130	146	146	146	146	146	146	142	7.502	2.2193	2.1653	2.6332
9	130	146	146	146	146	146	146	142	33.269	2.4992	2.7195	2.6332
10	130	146	146	146	146	146	146	142	56.619	2.9022	3.1317	2.6332
11	140	146	146	146	146	146	146	144.5	-51.305	8.7829	8.4861	7.9345
12	140	146	146	146	146	146	146	144.5	-40.432	8.2917	8.2535	7.9345
13	140	146	146	146	146	146	146	144.5	-17.334	7.4491	7.5564	7.9345
14	140	146	146	146	146	146	146	144.5	6.935	7.2072	7.3604	7.9345
15	140	146	146	146	146	146	146	144.5	30.992	7.6871	7.9664	7.9345
16	140	146	146	146	146	146	146	144.5	53.6	8.4367	8.5145	7.9345
17	150	146	146	146	146	146	146	147	-58.431	14.029	13.739	13.035
18	150	146	146	146	146	146	146	147	-48.184	13.966	13.611	13.035
19	150	146	146	146	146	146	146	147	-38.449	13.526	13.338	13.035
20	150	146	146	146	146	146	146	147	-27.49	12.984	12.943	13.035
21	150	146	146	146	146	146	146	147	-16.296	12.57	12.571	13.035
22	150	146	146	146	146	146	146	147	-4.938	12.342	12.352	13.035
23	150	146	146	146	146	146	146	147	6.494	12.329	12.369	13.035
24	150	146	146	146	146	146	146	147	17.896	12.527	12.617	13.035
25	150	146	146	146	146	146	146	147	29.171	12.915	13.004	13.035
26	150	146	146	146	146	146	146	147	40.238	13.41	13.396	13.035
27	150	146	146	146	146	146	146	147	51.045	13.836	13.665	13.035
28	160	146	146	146	146	146	146	149.5	-50.489	18.597	18.014	17.329
29	160	146	146	146	146	146	146	149.5	-36.792	18.051	17.6	17.329
30	160	146	146	146	146	146	146	149.5	-15.472	17.092	16.792	17.329
31	160	146	146	146	146	146	146	149.5	6.149	16.879	16.59	17.329
32	160	146	146	146	146	146	146	149.5	27.718	17.534	17.236	17.329
33	160	146	146	146	146	146	146	149.5	48.901	18.467	17.981	17.329
34	170	146	146	146	146	146	146	152	-52.533	21.793	21.099	20.331
35	170	146	146	146	146	146	146	152	-35.426	21.155	20.564	20.331
36	170	146	146	146	146	146	146	152	-14.824	20.27	19.739	20.331
37	170	146	146	146	146	146	146	152	5.882	20.123	19.54	20.331
38	170	146	146	146	146	146	146	152	26.569	20.837	20.183	20.331
39	170	146	146	146	146	146	146	152	47.124	21.707	20.98	20.331
40	180	146	146	146	146	146	146	154.5	-34.332	22.417	21.896	21.703
41	180	146	146	146	146	146	146	154.5	-14.327	21.623	21.076	21.703
42	180	146	146	146	146	146	146	154.5	5.679	21.555	20.883	21.703
43	180	146	146	146	146	146	146	154.5	25.685	22.34	21.511	21.703
44	180	146	146	146	146	146	146	154.5	45.691	23.158	22.331	21.703
45	180	146	146	146	146	146	146	154.5	65.694	23.177	22.522	21.703
46	180	180	180	180	180	180	180	180	15.68	25.269	25.954	26.635
47	180	180	180	180	180	180	180	180	25.68	25.607	26.411	26.635
48	180	180	180	180	180	180	180	180	45.69	26.321	27.366	26.635
49	180	180	180	180	180	180	180	180	65.694	26.604	27.589	26.635
50	180	180	180	180	180	180	180	180	-14.327	25.174	25.904	26.635
51	180	180	180	180	180	180	180	180	-34.332	26.061	26.859	26.635

TABLE S2. *ab-initio* calculated vs $^2J_{\text{Si-O-Si}}$ coupling model. The initial geometry was optimized with RHF/6-311G(d). Individual geometry, after structural constraint on Ω_0, Ω_k and ϕ, was not optimized. All Si-O bond distances were fixed to 1.6 Å and O-Si-O intra-tetrahedral angle set to 109.5°.

Index	$\Omega_0/1^\circ$	$\Omega_k/1^\circ$						$\overline{\langle\Omega\rangle}/1^\circ$	$\phi/1^\circ$	$^2J_{\text{Si-O-Si}}$-coupling /Hz		
		Ω_1	Ω_2	Ω_3	Ω_4	Ω_5	Ω_6			*ab-initio*	$J(\Omega_0, \overline{\langle\Omega\rangle}, \phi)$	$J(\Omega_0, \overline{\langle\Omega\rangle})$
52	120	120	120	120	120	120	120	120	8.237	-2.4502	-3.3223	-3.0199
53	120	130	130	130	130	130	130	127.5	8.237	-2.3752	-3.0189	-2.6976
54	120	140	140	140	140	140	140	135	8.237	-2.1224	-2.7155	-2.3753
55	120	146	146	146	146	146	146	139.5	8.237	-1.9657	-2.5334	-2.1819
56	120	150	150	150	150	150	150	142.5	8.237	-1.8819	-2.412	-2.0529
57	120	160	160	160	160	160	160	150	8.237	-1.6123	-2.1086	-1.7306
58	120	170	170	170	170	170	170	157.5	8.237	-1.2821	-1.8052	-1.4083
59	120	180	180	180	180	180	180	165	8.237	-1.083	-1.5017	-1.0859
60	130	120	120	120	120	120	120	122.5	7.5	1.4423	0.74504	1.1487
61	130	130	130	130	130	130	130	130	7.5	1.6351	1.2913	1.7196
62	130	140	140	140	140	140	140	137.5	7.5	1.9939	1.8376	2.2906
63	130	146	146	146	146	146	146	142	7.5	2.2193	2.1653	2.6332
64	130	150	150	150	150	150	150	145	7.5	2.3653	2.3838	2.8616
65	130	160	160	160	160	160	160	152.5	7.5	2.762	2.9301	3.4326
66	130	170	170	170	170	170	170	160	7.5	3.2326	3.4764	4.0035
67	130	180	180	180	180	180	180	167.5	7.5	3.6555	4.0226	4.5745
68	140	120	120	120	120	120	120	125	6.935	5.8964	5.2636	5.7602
69	140	130	130	130	130	130	130	132.5	6.935	6.2592	6.07	6.5965
70	140	140	140	140	140	140	140	140	6.935	6.8246	6.8765	7.4327
71	140	146	146	146	146	146	146	144.5	6.935	7.2072	7.3604	7.9345
72	140	150	150	150	150	150	150	147.5	6.935	7.4552	7.6829	8.269
73	140	160	160	160	160	160	160	155	6.935	8.0411	8.4894	9.1052
74	140	170	170	170	170	170	170	162.5	6.935	8.722	9.2958	9.9415
75	140	180	180	180	180	180	180	170	6.935	9.3362	10.102	10.778
76	150	120	120	120	120	120	120	127.5	6.494	10.354	9.6437	10.221
77	150	130	130	130	130	130	130	135	6.494	10.962	10.692	11.304
78	150	140	140	140	140	140	140	142.5	6.494	11.771	11.74	12.386
79	150	146	146	146	146	146	146	147	6.494	12.329	12.369	13.035
80	150	150	150	150	150	150	150	150	6.494	12.696	12.789	13.468
81	150	160	160	160	160	160	160	157.5	6.494	13.527	13.837	14.55
82	150	170	170	170	170	170	170	165	6.494	14.448	14.885	15.633
83	150	180	180	180	180	180	180	172.5	6.494	15.182	15.933	16.715
84	160	120	120	120	120	120	120	130	6.149	14.194	13.359	14.002
85	160	130	130	130	130	130	130	137.5	6.149	15.085	14.602	15.282
86	160	140	140	140	140	140	140	145	6.149	16.154	15.844	16.561
87	160	146	146	146	146	146	146	149.5	6.149	16.879	16.59	17.329
88	160	150	150	150	150	150	150	152.5	6.149	17.361	17.087	17.841
89	160	160	160	160	160	160	160	160	6.149	18.462	18.329	19.121
90	160	170	170	170	170	170	170	167.5	6.149	19.567	19.572	20.4
91	160	180	180	180	180	180	180	175	6.149	20.308	20.814	21.68
92	170	120	120	120	120	120	120	132.5	5.882	16.907	15.984	16.674
93	170	130	130	130	130	130	130	140	5.882	18.015	17.352	18.081
94	170	140	140	140	140	140	140	147.5	5.882	19.278	18.719	19.487
95	170	146	146	146	146	146	146	152	5.882	20.123	19.54	20.331
96	170	150	150	150	150	150	150	155	5.882	20.688	20.087	20.894
97	170	160	160	160	160	160	160	162.5	5.882	21.978	21.455	22.301
98	170	170	170	170	170	170	170	170	5.882	23.156	22.822	23.707
99	170	180	180	180	180	180	180	177.5	5.882	23.795	24.19	25.114
100	180	120	120	120	120	120	120	135	5.679	18.298	17.216	17.932
101	180	130	130	130	130	130	130	142.5	5.679	19.451	18.626	19.382
102	180	140	140	140	140	140	140	150	5.679	20.697	20.037	20.833
103	180	146	146	146	146	146	146	154.5	5.679	21.555	20.883	21.703
104	180	150	150	150	150	150	150	157.5	5.679	22.13	21.448	22.283
105	180	160	160	160	160	160	160	165	5.679	23.44	22.858	23.734
106	180	170	170	170	170	170	170	172.5	5.679	24.552	24.269	25.184
107	180	180	180	180	180	180	180	180	5.679	25.017	25.68	26.635

TABLE S3. *ab-initio* calculated vs $^2J_{\text{Si-O-Si}}$ coupling model. Individual geometry, after structural constraint on Ω_0 and Ω_k, was optimized using RHF/6-311G(d). The *ab-initio* J-coupling were then evaluated on the optimized geometry and compare with Eq. (19) of the main document. Excellent agreement in J-coupling model and *ab-initio* result is observed. All Si-O bond distances were fixed to 1.6 Å and O-Si-O intra-tetrahedral angle set to 109.5°.

Index	$\Omega_0/1^\circ$	$\Omega_k/1^\circ$						$\overline{\langle\Omega\rangle}/1^\circ$	$\phi/1^\circ$	$^2J_{\text{Si-O-Si}}$-coupling /Hz		
		Ω_1	Ω_2	Ω_3	Ω_4	Ω_5	Ω_6		optimized	*ab-initio*	$J(\Omega_0, \overline{\langle\Omega\rangle}, \phi)$	$J(\Omega_0, \overline{\langle\Omega\rangle})$
108	130	142	142	142	142	142	142	139	48.553	2.374	2.8141	2.4048
109	140	142	142	142	142	142	142	141.5	-3.63	7.1588	7.0094	7.6
110	150	142	142	142	142	142	142	144	-1.01	12.333	11.911	12.602
111	160	142	142	142	142	142	142	146.5	-48.131	18.823	17.438	16.817
112	170	142	142	142	142	142	142	149	-43.526	21.655	20.298	19.769
113	180	142	142	142	142	142	142	151.5	-163.34	22.695	21.663	21.123
114	130	146	146	146	146	146	146	142	-51.352	2.2449	3.0886	2.6332
115	140	146	146	146	146	146	146	144.5	69.457	8.2131	8.4749	7.9345
116	150	146	146	146	146	146	146	147	6.494	12.329	12.369	13.035
117	160	146	146	146	146	146	146	149.5	-43.389	18.997	17.832	17.329
118	170	146	146	146	146	146	146	152	-44.749	22.294	20.911	20.331
119	180	146	146	146	146	146	146	154.5	-158.46	23.025	22.07	21.703
120	130	149	149	149	149	149	149	144.25	-53.188	2.323	3.2866	2.8045
121	140	149	149	149	149	149	149	146.75	68.928	8.0614	8.7422	8.1853
122	150	149	149	149	149	149	149	149.25	-44.896	14.262	13.864	13.36
123	160	149	149	149	149	149	149	151.75	-40.024	19.09	18.109	17.713
124	170	149	149	149	149	149	149	154.25	-36.953	22.181	21.053	20.753
125	180	149	149	149	149	149	149	156.75	-63.423	24.16	22.994	22.138
126	120	178	178	178	178	178	178	163.5	-73.729	-0.84366	-0.80904	-1.1504
127	130	178	178	178	178	178	178	166	-69.237	4.3472	4.9844	4.4603
128	140	178	178	178	178	178	178	168.5	-69.038	10.709	11.248	10.61
129	150	178	178	178	178	178	178	171	-55.352	16.639	17.296	16.498
130	160	178	178	178	178	178	178	173.5	-40.144	21.178	21.882	21.424
131	170	178	178	178	178	178	178	176	-26.716	24.167	24.668	24.833
132	180	178	178	178	178	178	178	178.5	-142.29	25.249	25.956	26.345

TABLE S4. *ab-initio* calculated vs $^2J_{\text{Si-O-Si}}$ coupling model. The initial geometry was optimized with RHF/6-311G(d). Individual geometry, after structural constraint on Ω_0, Ω_k and ϕ, was not optimized. All Si-O bond distances were fixed to 1.6 Å and O-Si-O intra-tetrahedral angle set to 109.5°.

Index	$\Omega_0/1^\circ$	$\Omega_k/1^\circ$						$\overline{\langle\Omega\rangle}/1^\circ$	$\phi/1^\circ$	$^2J_{\text{Si-O-Si}}$-coupling /Hz		
		Ω_1	Ω_2	Ω_3	Ω_4	Ω_5	Ω_6			*ab-initio*	$J(\Omega_0, \overline{\langle\Omega\rangle}, \phi)$	$J(\Omega_0, \overline{\langle\Omega\rangle})$
133	140	140	140	140	130	130	130	136.25	6.935	6.5463	6.4733	7.0146
134	140	140	140	140	150	150	150	143.75	6.935	7.1414	7.2797	7.8508
135	140	140	140	140	160	160	160	147.5	6.935	7.4539	7.6829	8.269
136	140	140	140	140	170	170	170	151.25	6.935	7.7772	8.0862	8.6871
137	140	150	150	150	130	130	130	140	6.935	6.867	6.8765	7.4327
138	140	150	150	150	140	140	140	143.75	6.935	7.1414	7.2797	7.8508
139	140	150	150	150	160	160	160	151.25	6.935	7.7665	8.0862	8.6871
140	140	150	150	150	170	170	170	155	6.935	8.0846	8.4894	9.1052
141	150	130	146	146	146	146	146	145	6.494	11.882	12.09	12.747
142	150	140	146	146	146	146	146	146.25	6.494	12.129	12.264	12.927
143	150	150	146	146	146	146	146	147.5	6.494	12.47	12.439	13.107
144	150	160	146	146	146	146	146	148.75	6.494	12.848	12.614	13.288
145	150	170	146	146	146	146	146	150	6.494	13.223	12.789	13.468
146	120	154.5	153.24	142.43	158.36	134.56	157.87	142.62	47.643	-2.1903	-1.7321	-2.0478
147	130	157.08	153.88	145.05	160.56	135.83	157.46	146.23	50.461	2.3991	3.4132	2.9554
148	140	160.95	155.8	147.36	161.25	137.16	153.78	149.54	51.534	8.11	9.0703	8.4962
149	150	164.5	159.12	148.42	160.44	138.09	149.49	152.51	52.6	13.882	14.508	13.83
150	160	158.21	163.61	149.71	158.25	139.28	147.48	154.57	55.06	18.593	18.973	18.194
151	170	153.31	166.12	149.46	157.43	140.91	144.64	156.48	56.761	21.393	22.015	21.172
152	125	142	156	160	158	149	161	147	7.845	0.10924	0.060112	0.48901
153	135	142	156	160	158	149	161	149.5	7.2	4.9043	5.3085	5.8538
154	145	142	156	160	158	149	161	152	6.701	10.224	10.705	11.353

TABLE S4. ...continued. *ab-initio* calculated vs $^2J_{\text{Si-O-Si}}$ coupling model, continued. The initial geometry was optimized with RHF/6-311G(d). Individual geometry, after structural constraint on Ω_0, Ω_k and ϕ, was not optimized. All Si-O bond distances were fixed to 1.6 Å and O-Si-O intra-tetrahedral angle set to 109.5°.

Index	$\Omega_0/1^\circ$	$\Omega_k/1^\circ$						$\overline{\langle\Omega\rangle}/1^\circ$	$\phi/1^\circ$	$^2J_{\text{Si-O-Si}}$-coupling /Hz		
		Ω_1	Ω_2	Ω_3	Ω_4	Ω_5	Ω_6			*ab-initio*	$J(\Omega_0, \overline{\langle\Omega\rangle}, \phi)$	$J(\Omega_0, \overline{\langle\Omega\rangle})$
155	155	142	156	160	158	149	161	154.5	6.311	15.398	15.572	16.307
156	165	142	156	160	158	149	161	157	6.007	19.632	19.344	20.144
157	175	142	156	160	158	149	161	159.5	5.772	22.186	21.594	22.436
158	170	145	155	160	167	172	161	162.5	5.882	21.671	21.455	22.301
159	170	137	170	153	150.1	179.9	170	162.5	5.882	20.741	21.455	22.301
160	170	157	166	137	166	173	161	162.5	5.882	21.563	21.455	22.301
161	170	146	164	150	162	168	170	162.5	5.882	21.491	21.455	22.301
162	160	145	155	160	167	172	161	160	6.149	18.143	18.329	19.121
163	160	137	170	153	150.1	179.9	170	160	6.149	17.095	18.329	19.121
164	160	157	166	137	166	173	161	160	6.149	18.127	18.329	19.121
165	160	146	164	150	162	168	170	160	6.149	17.913	18.329	19.121
166	150	145	155	160	167	172	161	157.5	6.494	13.23	13.837	14.55
167	150	137	170	153	150.1	179.9	170	157.5	6.494	12.175	13.837	14.55
168	150	157	166	137	166	173	161	157.5	6.494	13.275	13.837	14.55
169	150	146	164	150	162	168	170	157.5	6.494	12.964	13.837	14.55
170	130	145	155	160	167	172	161	152.5	7.502	2.5666	2.9301	3.4326
171	130	137	170	153	150.1	179.9	170	152.5	7.502	1.8455	2.9301	3.4326
172	130	157	166	137	166	173	161	152.5	7.502	2.6513	2.9301	3.4326
173	130	146	164	150	162	168	170	152.5	7.502	2.3541	2.9301	3.4326
174	180	145	155	160	167	172	161	165	5.679	23.192	22.858	23.734
175	180	137	170	153	150.1	179.9	170	165	5.679	22.472	22.858	23.734
176	180	157	166	137	166	173	161	165	5.679	22.973	22.858	23.734
177	180	146	164	150	162	168	170	165	5.679	23.06	22.858	23.734
178	135	164	155	140	150	166	172	152.12	7.2	5.1271	5.5453	6.1002
179	145	164	155	140	150	166	172	154.62	6.701	10.523	11.031	11.691
180	155	164	155	140	150	166	172	157.12	6.311	15.748	15.976	16.723
181	165	164	155	140	150	166	172	159.62	6.007	19.973	19.804	20.617
182	175	164	155	140	150	166	172	162.12	5.772	22.458	22.084	22.939
183	127.5	135.6	142.8	161.2	155.4	147.3	169.8	145.89	7.668	1.1973	1.2069	1.6604
184	132.5	135.6	142.8	161.2	155.4	147.3	169.8	147.14	7.346	3.5995	3.8128	4.324
185	142.5	135.6	142.8	161.2	155.4	147.3	169.8	149.64	6.814	8.8003	9.1787	9.7959
186	152.5	135.6	142.8	161.2	155.4	147.3	169.8	152.14	6.399	13.998	14.183	14.89
187	162.5	135.6	142.8	161.2	155.4	147.3	169.8	154.64	6.076	18.462	18.233	19.01
188	172.5	135.6	142.8	161.2	155.4	147.3	169.8	157.14	5.825	21.434	20.87	21.695
189	120	168.34	168.34	168.34	169.06	169.06	169.06	156.53	-68.642	-0.50969	-1.0596	-1.4502
190	129.9	168.34	168.34	168.34	169.06	169.06	169.06	159	-63.499	4.9418	4.428	3.8716
191	130	172.78	172.78	172.78	173.11	173.11	173.11	162.21	-63.442	4.7433	4.7408	4.1717
192	140	177.8	177.8	177.8	177.24	177.24	177.24	168.14	-59.26	10.655	11.284	10.57
193	150	175.4	175.4	175.4	178.13	178.13	178.13	170.07	-57	17.058	17.172	16.365
194	160	179.1	179.1	179.1	177.75	177.75	177.75	173.82	-53.18	22.027	22.327	21.478
195	170	179.97	179.97	179.97	179.73	179.73	179.73	177.39	-51.021	25.272	25.957	25.093
196	180	178.58	178.58	178.58	178.68	178.68	178.68	178.97	-49.354	26.525	27.279	26.436
197	140	145	155	160	167	172	161	155	6.935	7.7815	8.4894	9.1052
198	140	137	170	153	150.1	179.9	170	155	6.935	6.8387	8.4894	9.1052
199	140	157	166	137	166	173	161	155	6.935	7.8553	8.4894	9.1052
200	140	146	164	150	162	168	170	155	6.935	7.5261	8.4894	9.1052

TABLE S5. *ab-initio* calculated vs $^2J_{\text{Si-O-Si}}$ coupling model from Sigma-2

Index	$\Omega_0/1^\circ$	$\Omega_k/1^\circ$						$\overline{\langle\Omega\rangle}/1^\circ$	$\phi/1^\circ$	$^2J_{\text{Si-O-Si}}$-coupling /Hz		
		Ω_1	Ω_2	Ω_3	Ω_4	Ω_5	Ω_6			*ab-initio*	$J(\Omega_0, \overline{\langle\Omega\rangle}, \phi)$	$J(\Omega_0, \overline{\langle\Omega\rangle})$
site 2-3	153.45	148.7	153.45	148.7	172.76	153.45	160.8	155.595	0.47	16.0	15.035	15.035
site 1-3	172	137.2	158.21	158.21	160.8	153.45	153.45	158.165	-0.45	22.07	20.958	20.958
site 4-1	137.2	158.21	172.26	158.21	148.78	152.04	148.74	151.575	0.0	6.48	6.552	6.552
site 4-2	148.74	137.2	148.74	152.04	148.74	153.45	153.45	148.8878	27.95	11.09	12.652	11.993